Int. J. Heat Mass Transfer. Vol. 26, No. 12, pp. 1783–1789, 1983
Printed in Great Britain

0017-9310/83 $3.00 + 0.00

THE EMITTER–RECEPTOR GEOMETRICAL CONFIGURATION INFLUENCE ON RADIATIVE HEAT TRANSFER

R. MIHAIL and GH. MARIA
Department of Chemical Engineering, Polytechnic Institute Bucharest, Polizu 1, 78126 Bucharest, Romania

(*Received* 13 *September* 1982 *and in final form* 13 *January* 1983)

Abstract—View factors or, equivalently, the direct interchange areas entering into Hottel's zone method, are computed numerically by procedures which give a fairly rapid solution. Some geometrical criteria are formulated with a view to enabling a choice of the most favourable configuration concerning the emitter–receptor radiative transfer. A number of examples for square, cubic, circular-cylinders and elliptical-cylinders support the results and the validity of the criteria proposed.

NOMENCLATURE

- A area of a surface zone [m^2]
- B the side of a square zone [m]
- E_i the black emissive power of zone i [W m^{-2}]
- $\overline{gg}$ the direct interchange area between a gas zone and another gas zone [m^2]
- $\overline{gs}$ the direct interchange area between a gas zone and a surface zone [m^2]
- k absorption factor of a volume zone [m^{-1}]
- L half length of a cylindrical zone [m]
- Q thermal flux [W]
- r space distance between two zones [m]
- R radius in a circle or current radius to the center in an ellipse [m]
- $\overline{sg}$ direct interchange area between a surface zone and a gas zone [m^2]
- $\overline{ss}$ direct interchange area between a surface zone and another surface zone [m^2]
- V volume [m^3]
- $\Delta x, \Delta y, \Delta z$ cartesian space distance [m]
- $\overline{Z_iZ_j}$ total interchange area between zone i and zone j [m^2].

Greek symbols

- $\hat{\theta}$ the angle between the direction of the radiation and the normal to a zone
- $\tau(r)$ transmittance along a beam path r.

1. INTRODUCTION

THERE are some important chemical processes (hydrocarbon pyrolysis, steam-cracking, hydrogen cyanide synthesis and others) which use radiant enclosures containing tubular reactors. The heat absorbed by the tubular endotherm reactor (receptor) proceeds from radiant walls and from combustion gases (emitters). The temperature distribution and heat fluxes in the enclosure are usually computed by the zone method, due to Hottel and Sarofim [1]. The radiant surfaces of receptors and emitters and the volume of radiant gases are divided into a number of surface and volume zones of convenient size. A most important element in the computing scheme is the assessment of view factors between the various zones. The view factors multiplied by A for an emitting surface and by $4kV$ for an emitting gas volume give the direct interchange areas. The total interchange area from an emitter i to a receptor j, $\overline{Z_iZ_j}$, characterises the ratio of the radiant energy emitted by zone Z_i which is absorbed by zone Z_j (directly or after multiple reflections), and of the total hemispherical emissive power of zone Z_i. A total energy balance for all zones of a closed radiant system results in the following set of nonlinear equations:

$$\sum_{i=1}^{n} \overline{Z_iZ_k}E_i - \left(\sum_{j=1}^{n} \overline{Z_kZ_j}\right)E_k = Q_k, \quad k = 1,2,\ldots,n \quad (1)$$

where Q_k represents the nonradiative heat flux leaving zone k. The solution to the system of equations (1) leads to the 3-dim. temperature field.

The general relationship given by Hottel and Sarofim [1] for the net radiative flux between the black zone 1 and the black zone 2,

$$Q_{1\rightleftharpoons 2} = \overline{s_1s_2}E_1 - \overline{s_2s_1}E_2, \quad (2)$$

shows that the increase of the direct interchange areas may be used for intensifying the thermal radiative transfer. It is clear that the value of the direct interchange area depends on the emitter–receptor geometry. For a given system some criteria may be formulated which enables a choice of the most favourable geometry concerning the emitter–receptor radiative transfer. It is the aim of the present paper to propose such criteria and to estimate the influence of the emitter–receptor geometry on the direct interchange areas.

2. ESTIMATION OF THE DIRECT INTERCHANGE AREAS

The radiation emitted by one zone in a closed radiative system containing a transparent medium is entirely received by the other zones of the system. In order to obtain the view factors the integration over every beam directed towards the receptor is required. The expressions for the direct interchange areas given by Hottel and Sarofim [1] are

$$\overline{s_i s_j} = \int_{A_i}\int_{A_j} \tau(r)\frac{\cos\hat{\theta}_i \cos\hat{\theta}_j}{\pi r^2}\,dA_i\,dA_j, \quad (3)$$

$$\overline{g_i s_j} = \int_{V_i}\int_{A_j} \tau(r)\frac{k_i \cos\hat{\theta}_j}{\pi r^2}\,dV_i\,dA_j, \quad (4)$$

$$\overline{g_i g_j} = \int_{V_i}\int_{V_j} \tau(r)\frac{k_i k_j}{\pi r^2}\,dV_i\,dV_j, \quad (5)$$

and direct analytical integration seems difficult even for a simple geometry. Hottel and Cohen [2] in some cases use graphical methods. Other authors, for instance Vercammen and Froment [3], Osuwan and Steward [4], use the Monte Carlo method, while Gross *et al.* [5] evaluate the integral by a series of additions of the integrand which can be carried out numerically in a simple way. Numerical methods involve more computational time, but they are justified; in a given closed system, the number of calculated integrals may be decreased taking into account three principles described in [1]: reciprocity ($\overline{s_1 s_2} = \overline{s_2 s_1}$), conservation ($\sum_j \overline{s_i s_j} = A_i$), and the Yamauti principle.

In the equations (3)-(5), $\tau(r)$ is the transmittance of the medium traversed by the radiation and it depends upon the beam length r and upon the absorption coefficient of the medium, k. A simple relationship is given by Hottel and Sarofim [1],

$$\tau(r) = \exp\left(-\int_0^r k\,dr\right). \quad (6)$$

Some details concerning the computation of the transmittance are available [1–3].

The evaluation of direct interchange areas for a number of characteristic cases, using various comparison criteria, is described below. In order to simplify the interpretation of results, a transparent medium ($\tau = 1$) is adopted as a first approximation, but the present analysis can readily be extended to the general situation where τ is given by the full equation (6). Figure 1 shows the results in their final form.

2.1. *Cubic and square zones*

For the radiative interchange between a surface square zone and a gas cubic zone, the detailed computational relations resulting from equations (3)–(5) are given by Hottel and Cohen [2]. It should be noticed that if the division of the space in the square zone is adequate for obtaining the temperature field in a radiant enclosure, it involves some geometrical approximations for cylindrical receptors. For these zones Simpson's rule of integration was applied with good results. The direct interchange area between squares contained in parallel planes (Fig. 1, the first example), calculated through this method is 0.199833, in comparison to 0.2 as calculated by Hottel and Sarofim [1].

2.2. *Finite right-circular cylindrical zones*

The numerical method of integration requires a uniform division of directions of integration. For a surface cylindrical zone (subscript 2) and a square zone

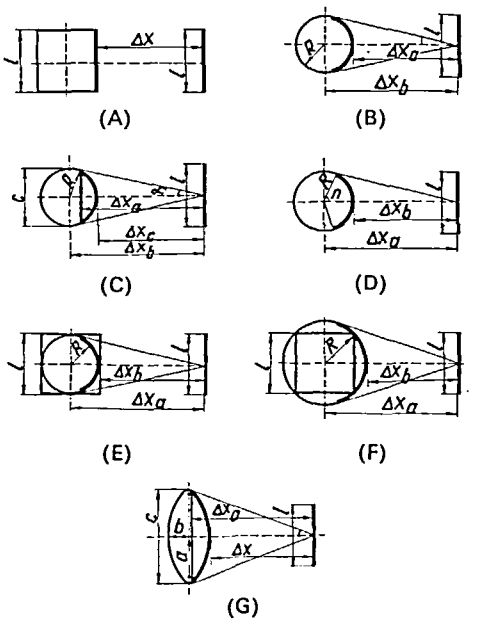

FIG. 1. (A) Right-square prism (l, $2L$) and parallel square (l). $l = 1$, $L = 0.5$, $\Delta x = 1$, $\overline{ss} = 0.199833$. (B) (a) Right-circular cylinder (R, $2L$) and parallel square (l). The area of the cross-section is constant and equal unit. $l = 1$, $L = 0.5$, $R = \sqrt{(l^2/\pi)} = 0.5641$. (i) $\Delta x_a = 1$, $\overline{ss} = 0.1656$; (ii) $\Delta x_b = 1$, $\overline{ss} = 0.3536$. (b) Right-circular cylinder (R, $2L$) and parallel square (l). The perimeter of the cross-section is constant. $l = 1$, $L = 0.5$, $R = 4l/(2\pi) = 0.6366$. (i) $\Delta x_a = 1$, $\overline{ss} = 0.1781$; (ii) $\Delta x_b = 1$, $\overline{ss} = 0.4102$. (C) (a) Right-circular cylinder (R, $2L$) and parallel square (l). The 'view angle' of the cross-section is constant. $l = 1$, $L = 0.5$, $\alpha = \arctan(l/2)$. (i) $R = 0.8090$, $\Delta x_c = 1$, $\overline{ss} = 0.2038$; (ii) $R = 0.4472$, $\Delta x_b = 1$, $\overline{ss} = 0.2650$. (b) Right-circular cylinder (R, $2L$) and parallel square (l). The 'view subtense' of the cross-section is constant and equal unit. $l = 1$, $L = 0.5$, $c = l$, $R = 0.5590$. (i) $\Delta x_a = 1$, $\overline{ss} = 0.2454$; (ii) $\Delta x_b = 1$, $\overline{ss} = 0.3497$. (D) Right-circular cylinder (R, $2L$) and parallel square (l). The 'view arc' of the cross-section is constant and equal unit. $l = 1$, $L = 0.5$, $R = 180l/2\pi n = 0.3885$. (i) $\Delta x_a = 1$, $\overline{ss} = 0.2176$; (ii) $\Delta x_b = 1$, $\overline{ss} = 0.1294$. (E) Right-circular cylinder (R, $2L$) and parallel square (l). The cylinder is inscribed in square prism (l, $2L$). $l = 1$, $L = 0.5$, $R = l/2 = 0.5$. (i) $\Delta x_a = 1$, $\overline{ss} = 0.3045$; (ii) $\Delta x_b = 1$, $\overline{ss} = 0.1534$. (F) Right-circular cylinder (R, $2L$) and parallel square (l). The cylinder is circumscribed in square prism (l, $2L$). $l = 1$, $L = 0.5$, $R = l/\sqrt{2} = 0.7071$. (i) $\Delta x_a = 1$, $\overline{ss} = 0.4616$; (ii) $\Delta x_b = 1$, $\overline{ss} = 0.1893$. (G) (a) Right-elliptical cylinder (a, b, $2L$) and parallel square (l). The area of the cross-section is constant and equal unit. $e = a/b$, $b = \sqrt{[l^2/(\pi e)]}$, $l^2 = \pi ab$, $L = 0.5$, $\Delta x = 1$, $l = 1$. (i) $e = 3.0$, $a = 0.9772$, $\overline{ss} = 0.2196$; (ii) $e = 2.0$, $a = 0.7978$, $\overline{ss} = 0.2102$; (iii) $e = 1.5$, $a = 0.6909$, $\overline{ss} = 0.1947$; (iv) $e = 1.4$, $a = 0.6675$, $\overline{ss} = 0.1899$; (v) $e = 1.3$, $a = 0.6432$, $\overline{ss} = 0.1850$. (b) Right-elliptical cylinder (a, b, $2L$) and parallel square (l). The perimeter of the cross-section is constant. $e = a/b$, $b = 4l/[\pi(e+1)]$, $4l = \pi(a+b)$, $L = 0.5$, $\Delta x = 1$, $l = 1$. (i) $e = 3.0$, $a = 0.9549$, $\overline{ss} = 0.2166$; (ii) $e = 2.0$, $a = 0.8488$, $\overline{ss} = 0.2178$; (iii) $e = 1.5$, $a = 0.7639$, $\overline{ss} = 0.2068$; (iv) $e = 1.4$, $a = 0.7427$, $\overline{ss} = 0.2026$; (v) $e = 1.3$, $a = 0.7196$, $\overline{ss} = 0.1981$. (c) Right-elliptical cylinder (a, b, $2L$) and parallel square (l). The 'view subtense' of the cross-section is constant and equal unit. $e = a/b$, $c = l$, $L = 0.5$, $\Delta x_a = 1$, $l = 1$. (i) $e = 3.00$, $a = 0.5065$, $\overline{ss} = 0.1821$; (ii) $e = 2.77$, $a = 0.5081$, $\overline{ss} = 0.1892$; (iii) $e = 2.54$, $a = 0.5096$, $\overline{ss} = 0.1970$. (d) Right-elliptical cylinder (a, b, $2L$) and parallel square (l). The 'view arc' of the cross-section is constant and equal unit. $e = a/b$, $L = 0.5$, $\Delta x = 1$, $l = 1$. (i) $e = 3.00$, $a = 0.5041$, $\overline{ss} = 0.1488$; (ii) $e = 2.54$, $a = 0.4832$, $\overline{ss} = 0.1515$; (iii) $e = 2.08$, $a = 0.4623$, $\overline{ss} = 0.1514$; (iv) $e = 1.85$, $a = 0.4494$, $\overline{ss} = 0.1475$; (v) $e = 1.62$, $a = 0.4342$, $\overline{ss} = 0.1389$.

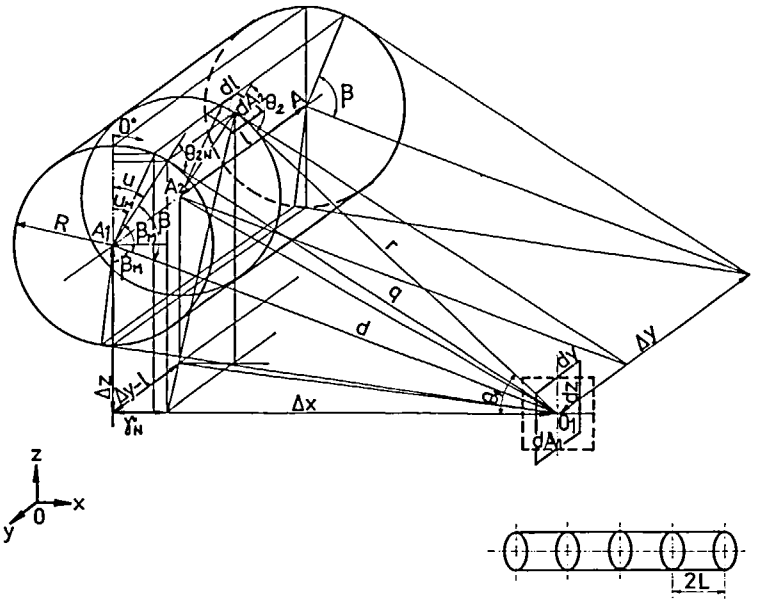

FIG. 2. A right-circular cylinder and a parallel or perpendicular square.

(subscript 1), at a space distance $(\Delta x, \Delta y, \Delta z)$ between their symmetry centers, the terms of equation (3) become (with the notation of Fig. 2)

$$dA_1 = (dy)(dz), \tag{7}$$

$$dA_2 = R(d\hat{\beta})(dl), \tag{8}$$

$$\cos \hat{\theta}_1 = (\Delta x - R \sin \hat{u})/r, \tag{9}$$

$$\cos \hat{\theta}_2 = (d \cos \hat{\beta} - R)/q/[1+(\Delta y - 1)^2/q^2]^{1/2}. \tag{10}$$

For a square the integral (3) is performed over the directions y and z and for a cylinder over the length l and the angle at center $\hat{\beta}$. Let n be the number of the current step upon the directions of integration; then the terms which appear in equations (7)-(10) are

$$\hat{\beta} = |-\hat{\beta}_M + n(\Delta\hat{\beta})|,$$

$$l = -L + n(\Delta l),$$

$$d = [(\Delta x)^2 + (\Delta z)^2]^{1/2},$$

$$q^2 = R^2 + d^2 - 2Rd \cos \hat{\beta},$$

$$\hat{u} = 180° - \arcsin(\Delta x/d) - \hat{\beta}_M + n(\Delta\hat{\beta}),$$

$$r^2 = (\Delta y - l)^2 + (\Delta x - R \sin \hat{u})^2 + (\Delta z + R \cos \hat{u})^2.$$

The subscript M designates the maximum value of angle $\hat{\beta}$, corresponding to the tangent at the cylinder.

The direct interchange area $\overline{ss}$ for a cylinder–parallel square system is

$$\overline{ss}_{(\text{parallel})} = \int_{-B/2}^{B/2}\int_{-B/2}^{B/2}\int_{-L}^{L}\int_{-\hat{\beta}_M}^{\hat{\beta}_M} \times e^{-\bar{k}r} \frac{R(d \cos \hat{\beta} - R)(\Delta x - R \sin \hat{u})}{\pi r^3 q[1+(\Delta y - l)^2/q^2]^{1/2}} \times (dy)(dz)(dl)(d\hat{\beta}) \tag{11}$$

and for a perpendicular arrangement

$$\overline{ss}_{(\text{perpendicular})} = \int_{-B/2}^{B/2}\int_{-B/2}^{B/2}\int_{-L}^{L}\int_{-\hat{\beta}_M}^{\hat{\beta}_M} \times e^{-\bar{k}r} \frac{R(\Delta y - l)(d \cos \hat{\beta} - R)}{\pi r^3 q[1+(\Delta y - l)^2/q^2]^{1/2}} \times (dx)(dz)(dl)(d\hat{\beta}). \tag{12}$$

For two parallel right-circular cylinders, with the notations in Fig. 3, equation (3) becomes

$$\overline{ss}_{(\text{parallel})} = \int_{-L_1}^{L_1}\int_{-L_2}^{L_2}\int_{-\hat{\beta}_{M_1}}^{\hat{\beta}_{M_1}}\int_{-\hat{\beta}_{M_2}}^{\hat{\beta}_{M_2}} \times e^{-\bar{k}r} \frac{R_1 R_2}{\pi r^2}\left[\frac{q_1 \cos \hat{\beta}_2 - R_2}{\mu^2}\right] \times \left\{\frac{(q_2 \cos \hat{\beta}_1 - R_1)}{[1+(\Delta y - l_1 - l_2)^2/\mu^2]}\right\}(dl_1)(dl_2)(d\hat{\beta}_1)(d\hat{\beta}_2) \tag{13}$$

where

$$\mu^2 = R_1^2 + q_2^2 - 2R_1 q_2 \cos \hat{\beta}_1,$$

$$r^2 = (\Delta y - l_1 - l_2)^2 + (\Delta x - R_1 \sin \hat{u}_1 - R_2 \sin \hat{u}_2)^2 + (\Delta z + R_1 \cos \hat{u}_1 + R_2 \cos \hat{u}_2)^2.$$

The case of radiative interchange between a surface right-circular cylindrical zone and a gas cubic zone yields

$$\overline{gs} = \int_{-B/2}^{B/2}\int_{-B/2}^{B/2}\int_{-B/2}^{B/2}\int_{-L}^{L}\int_{-\hat{\beta}_M}^{\hat{\beta}_M} \times \bar{k}\, e^{-\bar{k}r} \frac{R(d \cos \hat{\beta} - R)(dx)(dy)(dz)(dl)(d\hat{\beta})}{\pi r^2 q[(1+(\Delta y - 1)^2/q^2]^{1/2}}. \tag{14}$$

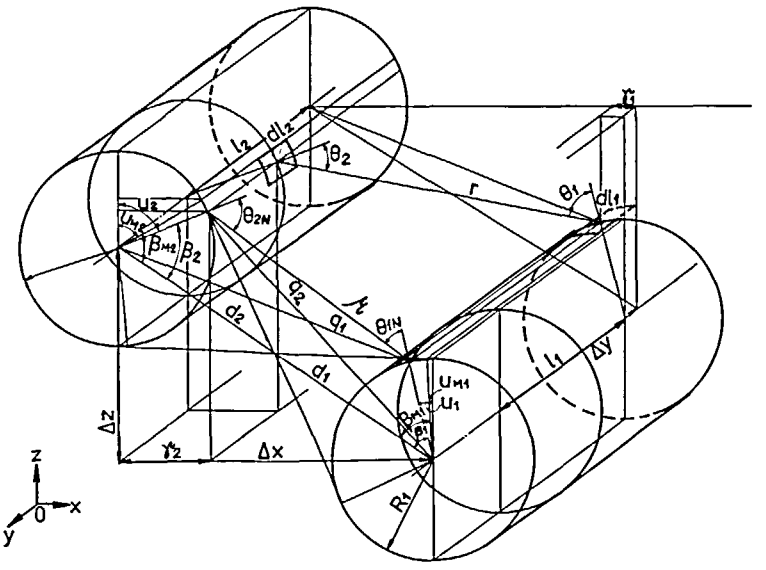

FIG. 3. Two parallel right-circular cylinders.

2.3. *Finite right-elliptical cylindrical zones*

This is a generalization of the above case for surface cylindrical zones. The direct interchange areas are calculated using a numerical technique and some elementary geometrical properties in order to simplify the computational procedure. Let us consider an infinitesimal external emitter located at a space distance $(\Delta x, \Delta y, \Delta z)$ from the symmetry center of the elliptical cylinder. First, in order to find the limits of integration, it is important to define the position of the tangents from this emitter point to the elliptical cross-section, which includes the emitter in its plane. In Fig. 4, the definition is given either by the angle at the center of the ellipse, $\hat{u}_M$, or by the distance to the focus, x, only one of the two definitions being necessary. The numerical procedure to find x starts with some proposed values comprised between the limiting values $(a-c, 2a-c)$, and verifies whether a stop-condition is satisfied. The half-interval search is used. The stop-condition from which one obtains x is

$$F(x)-(2c)^2 = 0$$

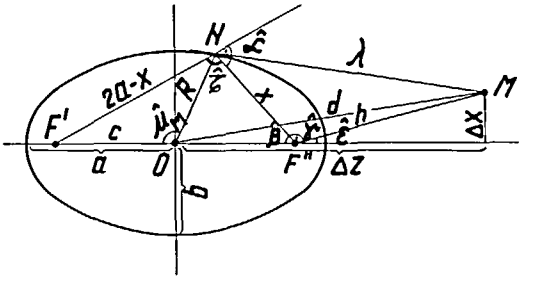

FIG. 4. The tangent from an external emitter point M to an ellipse. (The notation is used in equations (15)–(20) and in Appendix 1.)

where

$$F(x) = (2a-x)^2+x^2-2x(2a-x)\cos\hat{\tau}$$

and the angle $\hat{\tau}$ is computed as described in Appendix 1. The next step after the definition of the tangents is the estimation of the angle $\hat{u}_M$ and of the radius R_M, using Stewart's theorem (see Fig. 4)

$$R_M^2 = 2a^2+x^2-2ax-c^2, \tag{15}$$

$$\hat{u}_M = \arccos\left[\frac{c^2+R_M^2-(2a-x)^2}{2cR_M}\right]. \tag{16}$$

If $\hat{u}_{M_1}$ and $\hat{u}_{M_2}$ are the angles which define the two tangents from the emitter to the ellipse, the angle $\hat{\beta}_M$ results as

$$\hat{\beta}_M = (|\hat{u}_{M_1}-\hat{u}_{M_2}|)/2.$$

Integrating equations (3)–(5) leads after n steps $\Delta\hat{\beta}$ to the current values of the angles $\hat{u}, \hat{\beta}$ and of x and R

$$\hat{u} = \hat{u}_{M_1}+n(\Delta\hat{\beta}),$$

$$\hat{\beta} = |-\hat{\beta}_M+n(\Delta\hat{\beta})|,$$

$$R = (2a^2+x^2-2ax-c^2)^{1/2}$$

where x is a solution to the equation

$$f(x) = a^2-ax-c(2a^2+x^2-2ax-c^2)^{1/2}\cos\hat{u} = 0.$$

The radiating beam between the differential surface elements makes an angle $\hat{\theta}$ with the normal to the surface element of the ellipse dA; the term $\cos\hat{\theta}$ is contained in equations (3) and (4), and it is computed as in Appendix 2 (see the notations on Fig. 5),

$$\cos\hat{\theta} = \cos\hat{\theta}_N/[1+(\Delta y-l)^2/q^2]^{1/2}. \tag{17}$$

For an ellipse, the elliptical arc $d\hat{\beta}$ is approximated by

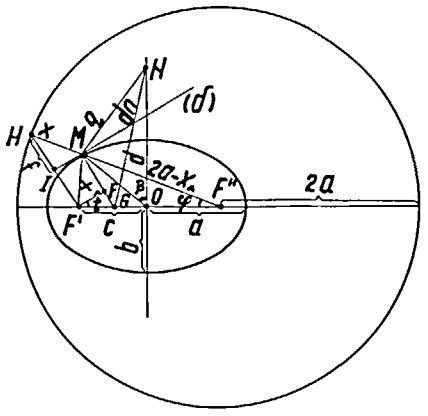

FIG. 5. Estimation of the term cos $\hat{\theta}$ for an elliptical cylinder. (The notation is used in equation (17) and in Appendix 2.)

that of a circle, so that the surface element of the ellipse is

$$dA \simeq R(d\hat{\beta})(dl). \quad (18)$$

Finally, the direct interchange area $\overline{ss}$ between an elliptical cylindrical surface and a parallel square, as shown in Fig. 6, is calculated by means of the relationship

$$\overline{SS}_{(\text{parallel})} = \int_{-B/2}^{B/2}\int_{-B/2}^{B/2}\int_{-L}^{L}\int_{-\hat{\beta}_M}^{\hat{\beta}_M} \times e^{-\bar{k}r}\frac{(\Delta x - R\sin\hat{u})R\cos\hat{\theta}}{\pi r^3} \times (dy)(dz)(dl)(d\hat{\beta}) \quad (19)$$

and for the case of their perpendicular arrangement

$$\overline{SS}_{(\text{perpendicular})} = \int_{-B/2}^{B/2}\int_{-B/2}^{B/2}\int_{-L}^{L}\int_{-\hat{\beta}_M}^{\hat{\beta}_M} \times e^{-\bar{k}r}\frac{(\Delta y - l)R\cos\hat{\theta}}{\pi r^3}(dx)(dz)(dl)(d\hat{\beta}). \quad (20)$$

The procedure to compute the integrals needed in the evaluation of direct interchange areas can be easily extended to other cases, such as: parallel or perpendicular elliptical cylinders, parallel or perpendicular elliptical and circular cylinders, elliptical cylinders and cubes, a.s.o.

3. RESULTS AND DISCUSSIONS

The multiple integrals which appear in equations (3)–(5) are calculated using Simpson's rule. A compromise is looked after between the precision of the integrals, which increases with the number of integration steps, and the computation time.

The comparison of direct interchange areas $\overline{ss}$, is done for the following cases of the emitter–receptor geometrical configurations: square–square prism, square–finite right-circular cylinder, square–finite right-elliptical cylinder, all in parallel space arrangement. The surface considered for the radiative interchange is located at the boundary of the prism or cylinder.

In order to simplify the calculation and the interpretation of results the following assumptions are adopted: (i) the space distance between zones $(\Delta x, \Delta y, \Delta z)$ is (1, 0, 0); (ii) the side of the square B or the length of the prism or of the cylinder $2L$ is equal to one; (iii) the gaseous medium is transparent.

The values of the integrals computed using equations (3)–(5) and shown in Fig. 1, reveal some possible geometrical criteria of comparison with respect to the performance of a given emitter–receptor shape. We only formulate some criteria for the prism and for the cylinders: the area or the perimeter of the cross-section is constant; the cylinder is inscribed or circumscribed in the prism; the 'view subtense' or the view arc of the cross-section is constant and equal with the side of square cross-section of the prism; the view angle of the cross-section is constant. In the above cases, reference is

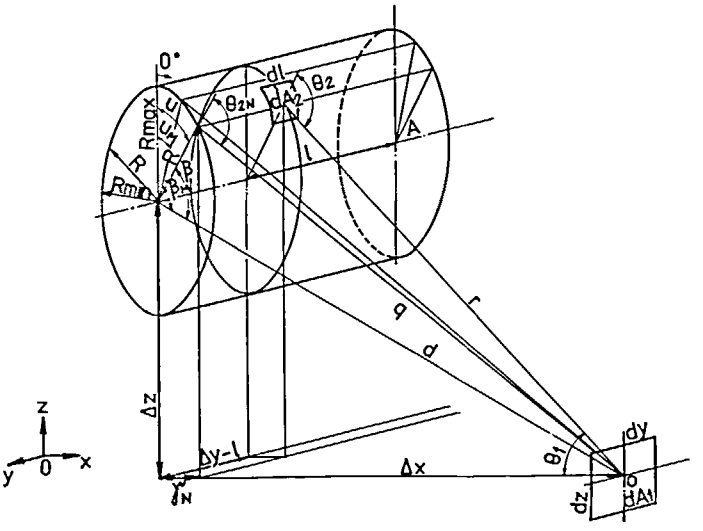

FIG. 6. A right-elliptical cylinder and a parallel or perpendicular square.

made respectively to the symmetry centers of the zones. The most adequate criterion for comparison in practical situations seems to be the constant view arc. The value of the integral $\overline{ss}$ for square–finite right-elliptical cylinder is intermediate between the values of square–right-square prism system and those of square–right-circular cylinder system, and is as much closer to the value of the circular cylinder as the semiaxis ratio of the elliptical cross-section is closer to one.

Therefore an elliptical shape of the tubular receptor may be favourable for the outside radiative heat transfer, but also for the inner heat transfer. Oliver and Karim [6] report a better arithmetic mean heat transfer coefficient for elliptical tubes. The improvement of the radiative or nonradiative transfer for elliptical tubes may be used for instance for the pyrolysis of hydrocarbons.

The procedure to estimate shape factors or, equivalently, the direct interchange areas, as described above, may be successfully applied to a solar receiver computation, for instance to the problem of Gross *et al.* [5]. The computational procedure, described in Section 2, which joins the well-known geometrical formulas and the numerical computational techniques, may give a more rapid solution to such problems and may be used for an optimal design of radiant enclosures.

REFERENCES

1. H. C. Hottel and A. F. Sarofim, *Radiative Transfer*. McGraw-Hill, New York (1967).
2. H. C. Hottel and E. S. Cohen, Radiant heat exchange in a gas-filled enclosure: allowance for non-uniformity of gas temperature, *A.I.Ch.E. Jl* **4**, 3 (1958).
3. H. A. J. Vercammen and G. F. Froment, An improved zone method using Monte Carlo techniques for the simulation of radiation in industrial furnaces, *Int. J. Heat Mass Transfer* **23**, 329 (1980).
4. S. Osuwan and F. Steward, A mathematical simulation of radiant heat transfer in a cylindrical furnace, *Can. J. Chem. Engng* **50**, 450 (1972).
5. U. Gross, K. Spindler and E. Hahne, Shapefactor-equations for radiation heat transfer between plane rectangular surfaces of arbitrary position and size with parallel boundaries, *Lett. Heat Mass Transfer* **8**, 219 (1981).
6. D. R. Oliver and R. B. Karim, Laminar-flow non-Newtonian heat transfer in flattened tubes, *Can. J. Chem. Engng* **49**, 236 (1971).
7. F. Dingeldey, *Coniques. Sistèmes de Coniques*. Gauthier-Villars-Leipzig, Paris (1944).

APPENDIX 1

THE COMPUTATION OF THE ANGLE $\hat{t}$

Using the notations in Fig. 4, the angle $\hat{t}$ is computed as follows:

$$d^2 = (\Delta x)^2 + (\Delta z)^2,$$

$$c^2 = a^2 - b^2,$$

$$h^2 = (\Delta x)^2 + (\Delta z - c)^2,$$

$$\hat{\beta} = \arccos[(c^2 - a^2 + ax)/(cx)],$$

$$\hat{\varepsilon} = \operatorname{arctg}[\Delta x/(\Delta z - c)],$$

$$\hat{\gamma} = 180° - \hat{\beta} - \hat{\varepsilon},$$

$$\lambda^2 = x^2 + h^2 - 2xh|\cos\hat{\gamma}|,$$

$$\hat{\alpha} = \arccos[(x^2 + \lambda^2 - h^2)/(2x\lambda)],$$

$$\hat{t} = 180° - 2\hat{\alpha}.$$

In the above formulas, the generalized Pitagora's theorem and a classical property of the tangents at an ellipse, described for instance by Dingeldey [7] are used. The case presented here is $\Delta z > a$; in other cases, the signs in the relationship of angle $\hat{\gamma}$ must be changed.

APPENDIX 2

THE COMPUTATION OF TERM $\cos\hat{\theta}$ OF EQUATIONS (3)–(5) FOR AN ELLIPTICAL CYLINDER

The angle $\hat{\theta}$ for an elliptical cylinder is defined in Section 2. To compute it, we use the notations in Fig. 5, the generalised Pitagora's theorem and Apollonius' property for an ellipse. Apollonius' property, given for instance by Dingeldey [7], specifies that the circle of radius $2a$ with the center in one of the foci of an ellipse, contains the symmetrical point of the other focus with respect to the tangent at the ellipse. So, the successive computational relationships are

$$f^2 = b^2x/(2a - x),$$

$$q^2 = R^2 + d^2 - 2Rd\cos\hat{\beta},$$

$$\hat{t} = \arccos[(f^2 + c^2 - a^2)/(2fc)] - 90°,$$

$$\overline{GO} = c - (x^2 - f^2)^{1/2}/\cos\hat{t},$$

$$d_n^2 = \overline{GO}^2 + d^2 - 2\overline{GO}d|\cos(\hat{\beta}_M + \hat{u}_M)|,$$

$$\overline{GM} = f + (x^2 - f^2)^{1/2}\tan\hat{t},$$

$$\cos\hat{\theta}_N = \left|\frac{d_n^2 - q^2 - \overline{GM}^2}{2q\overline{GM}}\right|,$$

$$\cos\hat{\theta} = \cos\hat{\theta}_N/[1 + (\Delta y - l)^2/q^2]^{1/2}.$$

INFLUENCE DE LA CONFIGURATION GEOMETRIQUE EMETTEUR-RECEPTEUR SUR LE TRANSFERT THERMIQUE PAR RAYONNEMENT

Résumé—Les facteurs géométriques ou les aires d'interchange direct entrant dans la méthode de zone de Hottel sont calculés numériquement par des procédures qui donnent une solution très rapide. Quelques critères géométriques sont formulés en vue de permettre un choix de la configuration la plus favorable concernant le transfert radiatif entre émetteur et récepteur. Un nombre d'exemples pour carré, cube, cylindre circulaire et cylindre elliptique apporte des résultats et justifie la validité des critères proposés.

DER EINFLUSS DER GEOMETRIE DES STRAHLERS UND EMPFÄNGERS AUF DEN STRAHLUNGSAUSTAUSCH

Zusammenfassung—Es wurden die Strahlungsformfaktoren mit numerischen Methoden berechnet, die sehr schnell konvergieren. Die Faktoren sind gleichbedeutend mit den direkten Austauschflächen, welche in die Zonenmethode nach Hottel eingehen. Im Hinblick auf die Auswahl der besten Anordnung für den Strahlungsaustausch zwischen Strahler und Empfänger werden einige geometrische Kriterien formuliert. Die Ergebnisse werden durch mehrere Beispiele für Quadrate, Würfel, Kreis, Zylinder und elliptischen Zylinder ergänzt und die Gültigkeit der angegebenen Kriterien nachgewiesen.

ВЛИЯНИЕ ВЗАИМНОГО РАСПОЛОЖЕНИЯ ИСТОЧНИКА И ПРИЕМНИКА ИЗЛУЧЕНИЯ НА ЛУЧИСТЫЙ ТЕПЛОПЕРЕНОС

Аннотация—Коэффициенты облученности, или эквивалентные им площади поверхностей взаимного лучистого обмена, используемые в зональном методе Хоттеля, рассчитываются численно на основе простой методики, которая позволяет довольно быстро получать решения. Сформулированы некоторые геометрические критерии выбора наиболее рационального взаимного расположения источника и приемника излучения для лучистого теплопереноса. На ряде примеров квадратной, кубической, кольцевой-цилиндрической и эллиптическо-цилиндрической конфигураций показана точность результатов и справедливость предложенных критериев.